MNRAS **000**, i–x (2016) Preprint 9 November 2016 Compiled using MNRAS LATEX style file v3.0

Identifying four *INTEGRAL* sources in the Galactic Plane via VLT/optical and *XMM-Newton*/X-ray spectroscopy⋆

Farid Rahoui,[1,2]† John. A. Tomsick,[3] and Roman Krivonos[4]
[1]*European Southern Observatory, Karl-Schwarzschild-Str. 2, D-85748 Garching bei München, Germany*
[2]*Harvard University, Department of Astronomy, 60 Garden street, Cambridge, MA 02138, USA*
[3]*Space Sciences Laboratory, 7 Gauss Way, University of California, Berkeley, CA, 94720-7450, USA*
[4]*Space Research Institute, Russian Academy of Sciences, Profsoyuznaya 84/32, 117997 Moscow, Russia*

arXiv:1611.02289v1 [astro-ph.HE] 7 Nov 2016

Accepted XXX. Received YYY; in original form ZZZ

ABSTRACT

We report on FORS2 spectroscopy aiming at the identification of four Galactic Plane sources discovered by *INTEGRAL*, IGR J18088−2741, IGR J18381−0924, IGR J17164−3803, and IGR J19173+0747, complemented by *XMM-Newton* spectroscopy for IGR J18381−0924. The presence of broad H I and He I emission lines and a flat Balmer decrement Hα/Hβ show that IGR J18088−2741 is a cataclysmic variable located beyond 8 kpc. For IGR J18381−0924, the detection of red-shifted Hα and O I emission signatures and the absence of narrow forbidden emission lines point towards a low-luminosity Seyfert 1.9 nature at $z = 0.031 \pm 0.002$. Its *XMM-Newton* spectrum, best-fit by an absorbed $\Gamma = 1.19 \pm 0.07$ power law combined with a $z = 0.026^{+0.016}_{-0.008}$ red-shifted iron emission feature, is in agreement with this classification. The likely IGR J17164−3803 optical counterpart is an M2III star at 3 to 4 kpc which, based on the X-ray spectrum of the source, is the companion of a white dwarf in an X-ray faint symbiotic system. Finally, we challenge the accepted identification of IGR J19173+0747 as an high mass X-ray binary. Indeed, the USNO optical counterpart is actually a blend of two objects located at the most likely 3 kpc distance, both lying within the error circle of the *Swift* position. The first is a cataclysmic variable, which we argue is the real nature of IGR J19173+0747. However, we cannot rule out the second one that we identify as an F3V star that, if associated to IGR J19173+0747, likely belongs to a quiescent X-ray binary.

Key words: X-rays: binaries – Stars: novae, cataclysmic variables – Stars: individuals: IGR J18088−2741 IGR J19173+0747, and IGR J17164−3803 – Galaxies: active – Galaxies: individual: IGR J18381−0924 – Techniques: spectroscopic

1 INTRODUCTION

Since its launch in 2002, the *INTErnational Gamma-Ray Astrophysics Laboratory* satellite (*INTEGRAL*, Winkler et al. 2003), has extensively monitored the hard X-ray sky with the Imager on-Board the *INTEGRAL* Satellite (IBIS, Ubertini et al. 2003). In the process, more than 600 *INTEGRAL* Gamma-Ray (IGR) sources were detected in the 20–100 keV energy range but many are still unidentified (see, e.g., Krivonos et al. 2012; Bird et al. 2016). Indeed, the large *INTEGRAL* positional uncertainty, typically 1–4′, makes the subsequent use of soft X-ray facilities such as the *Chandra X-ray Observatory* (Weisskopf et al. 2002) the *Swift* satellite (Gehrels et al. 2004), or the *X-ray Multi-Mirror-Newton* telescope (Jansen et al. 2001) compulsory to detect the soft X-ray counterparts, without the guarantee of unicity. Even in this case, the soft X-ray source may still be associated with several optical or near-infrared counterparts, some of them very faint, which precludes any definitive identification.

Comprehensive multi-wavelength observations are crucial to overcome this issue. This is the reason why several groups, including ours, are involved in large observational campaigns using multiple ground and space-based facilities with the goal of improving our view on hard X-ray emitters. So far, the majority of the new IGR sources that were identified are, as expected, active galactic nuclei (AGN). Nonetheless, an important result of the *INTEGRAL* surveys and subsequent multi-wavelength follow-ups have been the characterisation of a new population of peculiar persistent and transient supergiant X-ray binaries (SGXBs) in which a neutron star (NS) fed on the stellar winds of a blue supergiant through Bondi-Hoyle processes (see e.g. Negueruela et al. 2006; Tomsick et al. 2008; Chaty et al. 2008; Rahoui et al. 2008; Rahoui & Chaty 2008;

⋆ Based on observations performed with European Southern Observatory (ESO) Telescopes at the Paranal Observatory under programme ID 095.D-0972(A)

† E-mail: farid@rahoui.eu (FR)

© 2016 The Authors

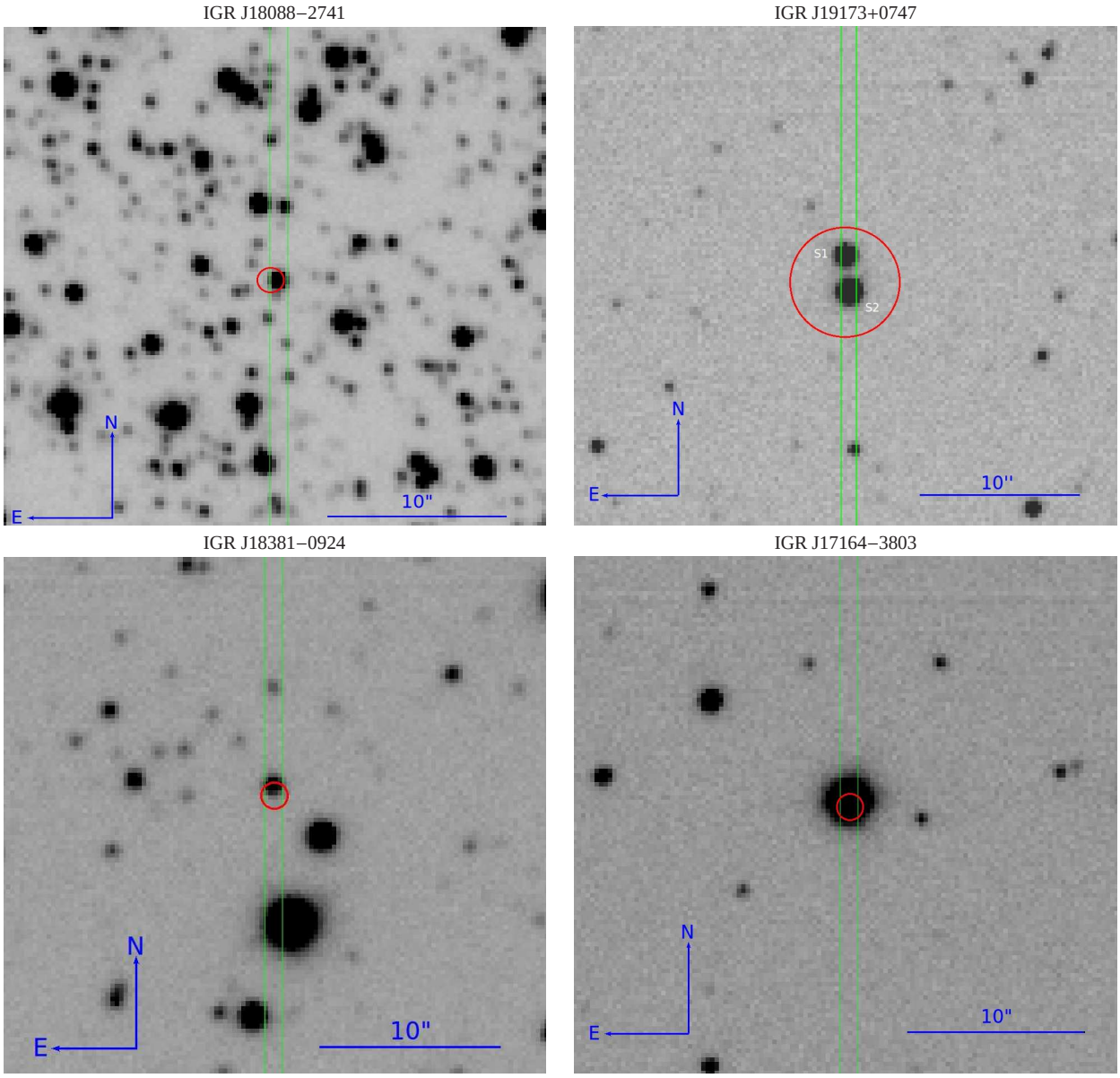

Figure 1. FORS2 *V* acquisition images of the four sources in our sample. *Chandra*/ACIS error circles (*Swift*/XRT in IGR J19173+0747 case) and the 1″ slit are superimposed.

Tomsick et al. 2012; Bodaghee et al. 2012; Chaty & Rahoui 2012; Coleiro et al. 2013). These discoveries significantly increased the number of known Galactic SGXBs and improved our understanding of their properties, although several unknowns remain, such as the origin of the erratic behaviour of transient SGXBs or the existence of a possible evolutionary link between the two populations. However, one of the most pressing issue is the absence of SGXBs hosting a black hole (BH) rather than a NS in the sample of newly-discovered sources. Such a phenomenon is puzzling, and it is not clear if it is due to formation and evolution processes (Belczynski & Ziolkowski 2009) or to the relatively low accretion power of BH-SGXBs, which makes them almost undifferentiated to isolated supergiant stars (see, e.g., Zhang et al. 2004; Casares et al. 2014; Munar-Adrover et al. 2014). In the era of the first ever detection of gravitational waves from a system of two colliding stellar-mass BHs (Abbott et al. 2016), a likely progenitor of which was a BH-SGXB, finding out if we can expect such systems to exist in high numbers in our own Galaxy is crucial.

Continuing with our ongoing campaign aiming at identifying newly-discovered hard X-ray sources, we report here on an optical spectroscopic study of three unidentified IGR sources, IGR J18088−2741, IGR J18381−0924, and IGR J17164−3803, which follows the discovery of their soft X-ray counterparts (Tomsick et al. 2016b,a). They were chosen because (1) they are located in the vicinity of the Galactic Plane; (2) their *Chandra* position was accurate enough to pinpoint their optical counterparts (see Figure 1); and (3) their X-ray spectra are hard and consistent with that expected from SGXB candidates. We added IGR J19173+0747, previously studied via soft X-ray and optical spectroscopy by Pavan et al. (2011) and Masetti et al. (2012), respectively, because it was tentatively classified as an HMXB but doubts remain. We present the data and their reduction in Section 2,

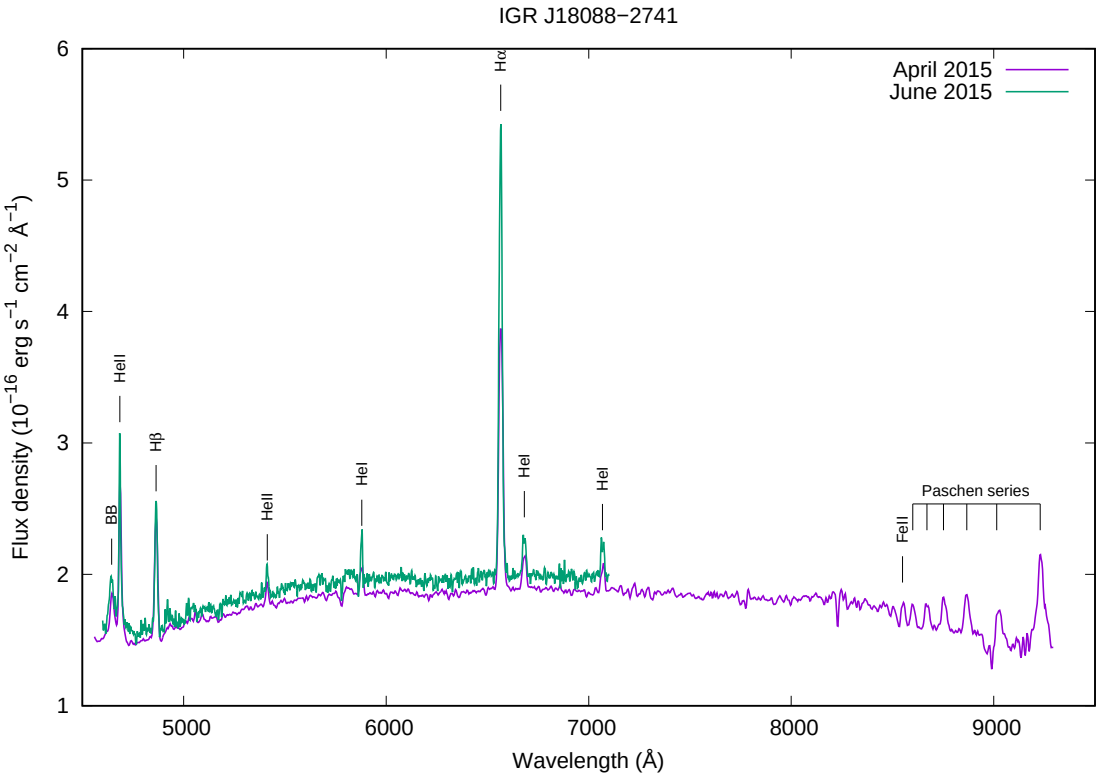

Figure 2. Flux-calibrated FORS2 spectrum of IGR J18088−2741 observed in April 2015 (magenta) and June 2015 (green). All the detected emission lines are marked. The most prominent telluric absorption troughs were manually removed.

whereas Section 3 is devoted to their analysis. We discuss the outcomes in Section 4 and conclude in Section 5.

2 OBSERVATIONS AND DATA REDUCTION

The dataset consists of (1) optical spectroscopy of the four sources with the FOcal Reducer/Low disperser Spectrograph 2 (FORS2, Appenzeller et al. 1998), mounted on the UT1 Cassegrain focus at the ESO Very Large Telescope (VLT) at Cerro Paranal; and (2) soft X-ray spectroscopy of IGR J18381−0924 with the PN-CCD and MOS-CCD cameras of the European Photon Imaging Camera (EPIC, Strüder et al. 2001; Turner et al. 2001) on board *XMM-Newton*.

2.1 Optical spectroscopy

On 2015 April 26, low-resolution spectroscopy of IGR J18088−2741, IGR J18381−0924, and IGR J17164−3803 was carried out with FORS2. The 300V and 300I grisms were used in combination with the GC435 and OG590 filters, respectively, for a total 4500 − 9300 Å spectral coverage. In both cases, the slit-width was set to 1″, giving a $R \sim 600 - 700$ average spectral resolution. Atmospheric conditions were relatively good, with a thin sky transparency, a seeing at 500 nm in the range 0.″6-0.″7, and an airmass always close to 1. Depending on the filters and photometric brightness of the sources, the exposure time of each individual frame ranged between 10 and 600 s and 2 exposures were taken per filter per source.

We also performed medium-resolution spectroscopy of IGR J18088−2741, IGR J18381−0924, and IGR J19173+0747 with FORS2 on 2015 June 27. We this time used the 600V and 600I grisms combined with the GC435 and OG590 filters, respectively, for a total 4500 − 9300 Å spectral coverage. The slit-width was set to 1″, giving a better $R \sim 1400$ average spectral resolution. Atmospheric conditions were similar, with a thin sky transparency, a seeing at 500 nm in the range 0.″5-0.″6, and airmass between 1.3 and 1.6. Individual exposure times were set from 200 to 600 s and 2 exposures were taken per filter per source.

In both April and June 2015, the A0V spectro-photometric standard star CD-32 9927 was observed in similar conditions for flux-calibration. We reduced the data using the dedicated pipeline (v. 5.3.5) implemented in the ESO data reduction environment `Reflex` v. 2.6 (Freudling et al. 2013). It follows the standard steps for optical spectroscopy reduction and produces cleaned, background-subtracted, and wavelength-calibrated 2D spectroscopic images. We then used the routines `apall`, `standard`, `sensfunc`, and `calibrate` implemented in `IRAF` v. 2.16[1] to optimally extract the source and spectro-phometric standard star 1D spectra, compute the sensitivity function, and apply it to the sources spectra for flux calibration.

Table 1. Optical lines in IGR J18088−2741 2015 April and June FORS2 spectra. Note that June spectrum beyond 7100 Å was contaminated by clouds and we decided not the measure the lines, which were however present.

		April 2015			June 2015		
Element	λ_c[a]	$\mathring{W}$[b]	FWHM[c]	F_{line}[d]	$\mathring{W}$	FWHM	F_{line}
BB	4645	−7.2 ± 0.4	2010±135	1.14±0.05	−10.6±0.6	2732 ± 199	1.60±0.10
He II	4686	−12.6±0.2	666±72	1.86±0.06	−10.5 ± 0.3	586 ± 38	1.66 ± 0.09
Hβ	4861	−10.7±0.3	705±51	1.65±0.04	−9.7 ± 0.3	786 ± 43	1.51 ± 0.09
He II	5409	−1.5±0.2	551±72	0.26±0.03	−1.6 ± 0.2	524 ± 75	0.32±0.04
He I	5875	−3.0±0.4	353±57	0.55±0.08	−2.7 ± 0.3	430 ± 37	0.53 ± 0.05
Hα	6561	−26.7±0.2	652±45	5.05±0.05	−32.4 ± 0.1	769 ± 37	6.51 ± 0.05
He I	6678	−3.3±0.2	804±92	0.62±0.04	−3.1 ± 0.3	825 ± 74	0.62 ± 0.07
H I	7065	−2.4±0.2	699±74	0.51±0.04	−2.9 ± 0.4	662 ± 66	0.57 ± 0.08
H I	8543	−2.8±0.3	401±51	0.45±0.04	–	–	–
H I	8597	−2.9±0.3	377±40	0.46±0.05	–	–	–
H I	8663	−3.2±0.3	402±39	0.51±0.05	–	–	–
H I	8749	−4.4±0.2	437±30	0.70±0.04	–	–	–
H I	8862	−5.4±0.3	507±39	0.84±0.04	–	–	–
H I	9015	−6.3±0.4	420±51	0.72±0.05	–	–	–
H I	9228	−13.4±1.0	520±107	2.08±0.20	–	–	–

[a] Measured wavelength in Å
[b] Equivalent widths in Å
[c] Full-width at half-maximum in km s^{-1}, quadratically corrected for instrumental broadening
[d] Intrinsic line flux in units of 10^{-15} erg cm^{-2} s^{-1}

2.2 *XMM-Newton* observation of IGR J18381−0924

An observation of IGR J18381−0924 with *XMM-Newton* occurred on 2016 March 19 between 12.5 h and 20.5 h UT. The PN, MOS1, and MOS2 instruments were all operated in Full Frame mode with the medium blocking filter, yielding exposure times of 24, 28, and 28 ks, respectively. We previously identified IGR J18381−0924 with the *Chandra* source CXOU J183818.5–092552 (Tomsick et al. 2016b), and we detect a source with a consistent position in the *XMM-Newton* data.

We reduced the data using the *XMM-Newton* Science Analysis Software (SAS) v14.0.0 and the 2015 September 2 version of the instrument calibration files. We filtered the PN event list to select good events using the #XMMEA_EP criterion and included single and double events ("PATTERN<=4"). For the MOS event lists, we also selected good events using #XMMEA_EM but included single through quadruple events ("PATTERN<=12") as recommended based on the SAS Data Analysis Threads[2].

To extract the energy spectra, we used a circular region centred on the source with a radius of 35″. We made background spectra by extracting events from rectangular regions of the detector that are free of sources. We binned the 0.3–12 keV PN spectrum by requiring a signal-to-noise ratio of at least 5 in each bin and required a signal-to-noise >3 for the 0.3–10 keV MOS spectra. After background subtraction, we obtained PN, MOS1, and MOS2 count rates of 0.248 ± 0.004, 0.077 ± 0.002, and 0.083 ± 0.002 count/s, respectively.

[1] `IRAF` is distributed by the National Optical Astronomy Observatories, which are operated by the Association of Universities for Research in Astronomy, Inc., under cooperative agreement with the National Science Foundation.
[2] See http://www.cosmos.esa.int/web/xmm-newton/sas-threads

3 RESULTS AND ANALYSIS

In the following, we summarise the main properties of the four sources as they were known before the present study and we give some insights on the most likely nature of their optical counterparts.

3.1 IGR J18088−2741

IGR J18088−2741 was first reported in Krivonos et al. (2012), and Tomsick et al. (2016b) later identified it as CXOU J180839.8−274131 with *Chandra*. The fit to its combined *Chandra* and *INTEGRAL* spectra with a cut-off power law yields a very hard $\Gamma \approx -1.5$ and $E_{fold} \approx 4.8$ keV, whereas the column density is $N_H < 7 \times 10^{21}$ cm^{-2}. The authors also find a 800 to 950 s modulation in its *Chandra* light curve (although this was based on coverage of only five cycles of the modulation) and the 0.″74 *Chandra* positional accuracy led to an unambiguous association of IGR J18088−2741 with VVV J180839.77−274131.7 (Vista Variables in the Via Lactea catalogue, Minniti et al. 2010). The reported magnitudes of the source are $Z = 16.77 \pm 0.06$, $Y = 16.65 \pm 0.07$, $J = 16.09 \pm 0.06$, $H = 15.82 \pm 0.08$, and $K_S = 15.67 \pm 0.09$, which yields a flux density of about 1.7×10^{-16} erg cm^{-2} s^{-1} at 0.88 μm compared to about 1.5×10^{-16} erg cm^{-2} s^{-1} for the continuum level of our first FORS2 spectrum. This infrared counterpart is also that of OGLE-BLG-RRLYR-14363, a variable star with a 0.28 days orbital period listed in the Optical Gravitational Lensing Experiment Catalogue of Variable Stars (OGLE-III, Soszyński et al. 2011). We note that the Vista source is also variable and a comparison of the phase-folded OGLE/I and VVV/K_S light curves (Figure 3) unambiguously shows that these variations are due to orbital modulation.bb

Based on its very hard cut-off power law X-ray spectrum, the possible presence of pulse period, as well as the very short orbital period, Tomsick et al. (2016b) classified IGR J18088−2741 as a likely intermediate polar (IP), i.e. a magnetised cataclysmic variable (CV); our FORS2 optical spectra concur with this statement (see Figure 2; note that we do not display the red part of the June

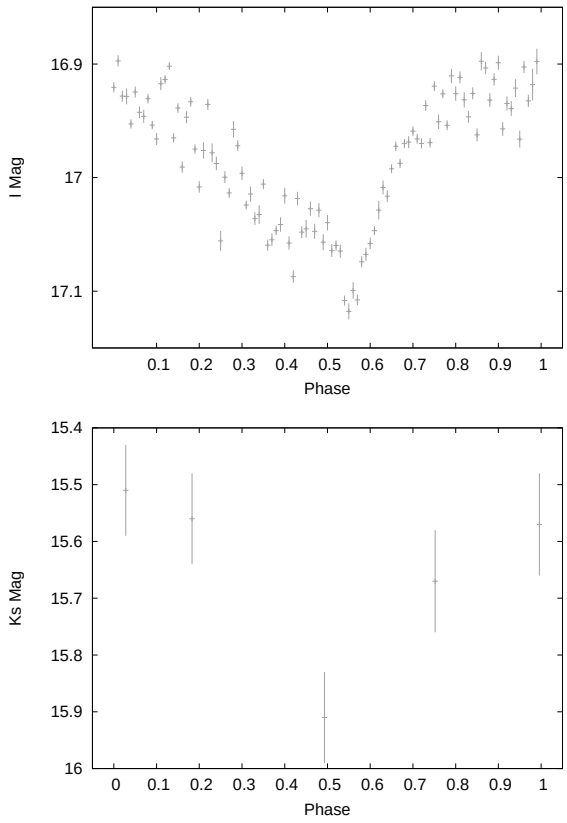

Figure 3. Top: Phase-folded I band OGLE light curve of IGR J18088−2741. **Bottom** Phase-folded K_S band VVV light curve of IGR J18088−2741. Note that the phase-folding is such that the time of maximum brightness occurs at phase 0 but this is arbitrary.

spectrum as it was contaminated by passing clouds and many narrow absorption troughs not related to the source were present). Indeed, the optical light is dominated by strong emission signatures of H I (Balmer and Paschen series) and He I, which, along with the detection of the Bowen Blend around 4640 Å and He II at 4686 Å, point towards the presence of an irradiated accretion disc. Moreover, if the continuum and most of the emission lines are constant between April and June observations, the Bowen Blend and Hα are a notable exception, with a flux increase between the two epochs. This may hint at orbital modulations and a brightening of the hot spot of the accretion disc.

Centred at 5779 Å, we also report a Diffuse Interstellar Band (DIB) whose equivalent width is known to correlate well with the extinction along the line-of-sight of the sources for which it is detected (Jenniskens & Desert 1994). Averaging out DIB5779 equivalent width values found in April and June spectra, i.e. $\mathring{W} = 0.65 \pm 0.06$ Å and $\mathring{W} = 0.53 \pm 0.11$ Å, respectively, we find that IGR J18088−2741 suffers from an ISM extinction $E(B-V) = 0.96 \pm 0.10$ along its line-of-sight, i.e. $A_V = 2.98 \pm 0.31$ for $R_V = 3.1$. Using the 3D extinction map built in Marshall et al. (2006), we find that it is consistent with a distance to the source $D \geq 9$ kpc. The more recent 3D extinction map of Green et al. (2015) gives a similar value, with $D \geq 8$ kpc. Moreover, correcting both spectra using the extinction law given in Fitzpatrick (1999), we estimate that the Balmer decrement Hα/Hβ is about 1.02 and 1.47 in April and June, respectively, i.e. consistent with unity as expected for Balmer lines originating from the optically thick accretion disc in CVs (Williams 1980; Tomsick et al. 2016b).

Table 2. Optical lines in IGR J19173+0747-S1 June 2015 FORS2 spectra.

Element	λ_c [a]	$\mathring{W}$ [b]	FWHM [c]	F_{line} [d]
BB	4641	−7.3 ± 0.8	1974 ± 307	1.81±0.20
He II	4685	−10.8 ± 0.6	841 ± 74	2.70 ± 0.13
Hβ	4861	−9.0 ± 0.3	731 ± 41	2.39 ± 0.08
He I	4921	−1.0 ± 0.2	423 ± 83	0.27±0.05
He I	5015	−1.1 ± 0.2	691 ± 139	0.32±0.05
He II	5409	−1.7 ± 0.2	935 ± 133	0.63±0.08
He I	5876	−3.2 ± 0.3	606 ± 38	1.29 ± 0.09
Hα	6561	−19.1 ± 0.1	562 ± 26	7.92 ± 0.06
He I	6678	−2.0 ± 0.2	462 ± 40	0.81 ± 0.07
H I	7065	−1.5 ± 0.2	440 ± 48	0.64 ± 0.08
H I	8543	−1.7±0.4	493±62	0.69±0.08
H I	8599	−1.1±0.2	286±40	0.41±0.07
H I	8667	−2.0±0.3	424±43	0.75±0.07
H I	8752	−2.2±0.4	467±47	0.84±0.08
H I	8862	−3.7±0.4	809±90	1.41±0.15
H I	9016	−4.1±0.4	635±60	1.52±0.12
H I	9228	−6.0±0.9	616±41	2.21±0.20

[a] Measured wavelength in Å
[b] Equivalent widths in Å
[c] Full-width at half-maximum in km s^{-1}, quadratically corrected for instrumental broadening
[d] Intrinsic line flux in units of 10^{-15} erg cm^{-2} s^{-1}

3.2 IGR J19173+0747

IGR J19173+0747 was first reported in Pavan et al. (2011), in which the authors investigated the presence of unknown sources in the vicinity of AX J1910.7+0917 *INTEGRAL* field-of-view. They performed a fit to its 17–80 keV ISGRI spectrum and found that it was best-described by a $\Gamma = 3.3^{+0.9}_{-0.7}$ power law. The follow-up observations with the X-Ray Telescope (XRT, Burrows et al. 2005) on board the *Swift* satellite led to the identification of its soft X-ray counterpart, the 0.5–10 keV spectrum of which was best-fit with a $\Gamma = 0.6 \pm 0.2$ power law, pointing towards a break in the 10–20 keV energy range and/or variability. Moreover, the 3.″4 positional accuracy of the *Swift*/ observation allowed Pavan et al. (2011) to associate IGR J19173+0747 with USNOB1.0 0977−0532587 and 2MASS J19172078+0747506. Masetti et al. (2012) subsequently reported on optical spectroscopy of the optical counterpart and concluded that IGR J19173+0747 was a likely HMXB based on its X-ray properties and the sole detection of an Hα emission line in its optical spectrum. Our results however contradict this statement.

Indeed, as shown in the top-right panel of Figure 1, which displays the V band FORS2 acquisition image of IGR J19173+0747, what is classified as a single point source in both USNO and 2MASS catalogues actually consists of two objects. They are separated by about 2.2″ and are well within the *Swift* error circle, meaning that both are potential optical counterparts to IGR J19173+0747. We labelled the northern source S1 and the southern one S2 and Figure 4 displays their FORS2 spectra; we also report the measurements of S1's detected lines in Table 2. S1 spectrum strongly resembles that of IGR J18088−2741, with a wealth of H I and He I emission lines as well as the presence of the Bowen Blend and He II λ4686. This similarity, combined with the fact that its 0.5-80 keV spectrum is likely best-described by a hard cut-off power law, suggests that S1 is the optical counterpart to a CV and that we observe the optically thick accretion disc. This

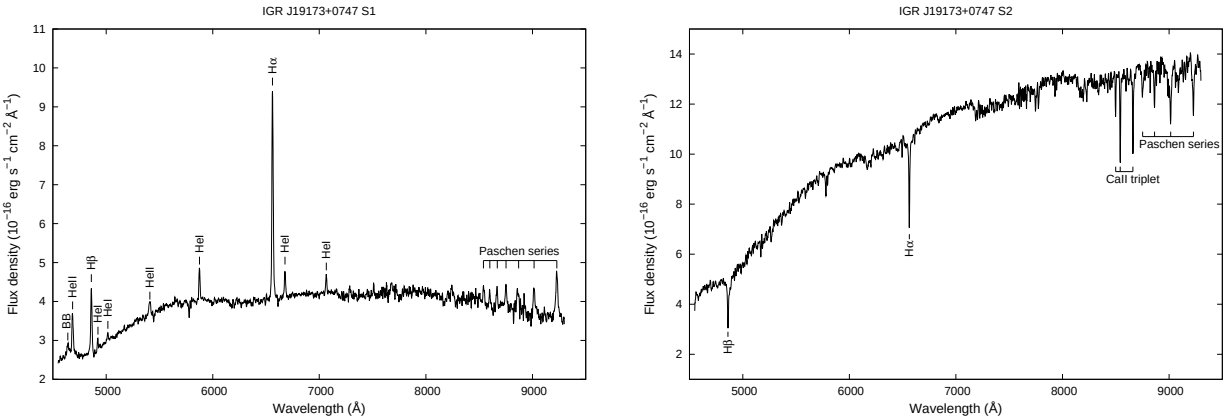

Figure 4. Flux-calibrated FORS2 spectra of the two possible optical counterparts to IGR J19173+0747, a likely CV (S1, left) and an F3 V star (S2, right). All the detected lines are marked. The most prominent telluric absorption troughs were manually removed.

statement is further strengthens by the fact that the Balmer decrement is Hα/H$\beta\approx$0.96, i.e. close to unity as expected for CVs. We assessed this decrement using the measured ISM extinction along S1 line-of-sight, $A_{\rm V} = 3.35 \pm 0.50$, derived from the equivalent width of DIB5779, $\mathring{W} = 0.70 \pm 0.09$ Å, using the relationship given in Jenniskens & Desert (1994). Incidentally, this extinction yields a distance between 3 and 5 kpc using the 3D extinction map given in Marshall et al. (2006), and between 1.5 and 2.9 kpc using the work of Green et al. (2015).

In contrast to S1, S2 spectrum is dominated by absorption signatures of Hα, Hβ, Paschen lines at 8752 Å, 8864 Å, 9017 Å and 9230 Å, as well as the Ca II triplet at 8498 Å 8542 Å, and 8662 Å. Comparing it to the optical spectra provided in the STELIB library (Le Borgne et al. 2003), we identify S2 as a likely F3 V star. DIB5779 is also present in its spectrum and we measure its equivalent width to be $\mathring{W} = 0.75 \pm 0.08$ Å, which results in an ISM extinction $A_{\rm V} = 3.60 \pm 0.47$ and a distance between 3 and 5 kpc. This means that S2 suffers from the same ISM extinction and is located at the same distance as S1, which may hint at both belonging to the same group of stars.

3.3 IGR J18381−0924

Similarly to IGR J18088−2741, IGR J18381−0924 was first reported in Krivonos et al. (2012) and studied in more details in Tomsick et al. (2016b) via both *Chandra* and *INTEGRAL* X-ray spectroscopy. The authors showed that the source had a relatively hard spectrum consistent between ACIS-I and ISGRI, with a best-fit power law $\Gamma = 1.4 \pm 0.1$ and $N_{\rm H} = 3.8^{+0.9}_{-0.7} \times 10^{22}$ cm^{-2}. The 0.″74 *Chandra* pointing accuracy allowed for the identification of two possible near-infrared counterparts to the source in the UKIDSS Galactic Plane Survey (UGPS, Lucas et al. 2008), UGPS J183818.58-092552.9 and UGPS J183818.59-092551.8, both classified as galaxies with reported K magnitudes 13.035 ± 0.003 and 12.833 ± 0.002.

In the optical however, as shown in Figure 1, only UGPS J183818.59-092551.8 is detected. Our FORS2 spectra, obtained in April and June 2015 (Figure 5, magenta and green, respectively) confirm its classification as extragalactic. Indeed, we only detect red-shifted emission signatures of Hα and O I at 8446 Å, which yields a red shift $z = 0.031 \pm 0.002$ (Table 3). The source is also variable and the continuum is twice as bright in June compared to April. Measurements show that the two emission lines, relatively broad with FWHMs of about 2000–2600 km s^{-1} for Hα and 1600 km s^{-1} for O I, also brightened at constant equivalent widths, pointing towards a common origin with the continuum.

DIB5779 is also present, and its equivalent width $\mathring{W} = 1.20 \pm 0.15$ Å results in an extinction along the line-of-sight of the source $A_{\rm V} = 5.75 \pm 0.85$. We note that this extinction, equivalent to $N_{\rm H} = (1.27 \pm 0.19) \times 10^{22}$ cm^{-2} using the relationship given in Güver & Özel (2009), is consistent with the total Galactic extinction of about 1.25×10^{22} cm^{-2} as obtained with the tool provided in the *Chandra* website[3].

In the X-ray domain, similarly to what was done for the *Chandra* spectrum (Tomsick et al. 2016b), we fit the PN, MOS1, and MOS2 *XMM-Newton* spectra of IGR J18381−0924 with an absorbed power law. In modelling the absorption, we assumed Wilms et al. (2000) abundances and Verner et al. (1996) cross sections. We also included a multiplicative constant factor to account for possible normalisation differences between instruments. With a PN constant fixed to 1.0, we find 1.00 ± 0.05 and 0.96 ± 0.04 (90% confidence errors) for MOS1 and MOS2, respectively, indicating that there are no significant normalisation differences. With the model Constant×Tbabs×Pegpwrlw, we obtain $\chi^2/\nu = 635/585$ and see significant residuals between 6 and 7 keV (see Figure 6, middle panel, for the residuals). Adding a Gaussian emission line improves the fit to $\chi^2/\nu = 582/582$, and the central energy is $6.24^{+0.05}_{-0.09}$ keV, pointing towards a red-shifted iron line (see Figure 6, top and bottom panels, for the best-fit and residuals, respectively, as well as Table 4, second column, for the best-fit parameters). If we assume a rest energy of 6.4 keV, i.e. the presence of neutral iron as expected for an AGN, the inferred red shift is $z = 0.026^{+0.016}_{-0.008}$, which is consistent with the value measured from the optical spectrum of UGPS J183818.59-092551.8, proving that it is the proper optical counterpart to IGR J18381−0924. The width of the line is $\sigma = 0.15^{+0.18}_{-0.07}$ keV, and the equivalent width is 280^{+130}_{-80} eV. The spectral parameters also indicate a photon index $\Gamma = 1.19 \pm 0.07$ and a column density of $(2.21 \pm 0.16) \times 10^{22}$ cm^{-2}. The latter is in excess of the total ISM extinction along the line-of-sight of the source as well as that derived from DIB5779, which hints at the presence of a local absorbing medium. We also note

[3] http://cxc.harvard.edu/toolkit/colden.jsp

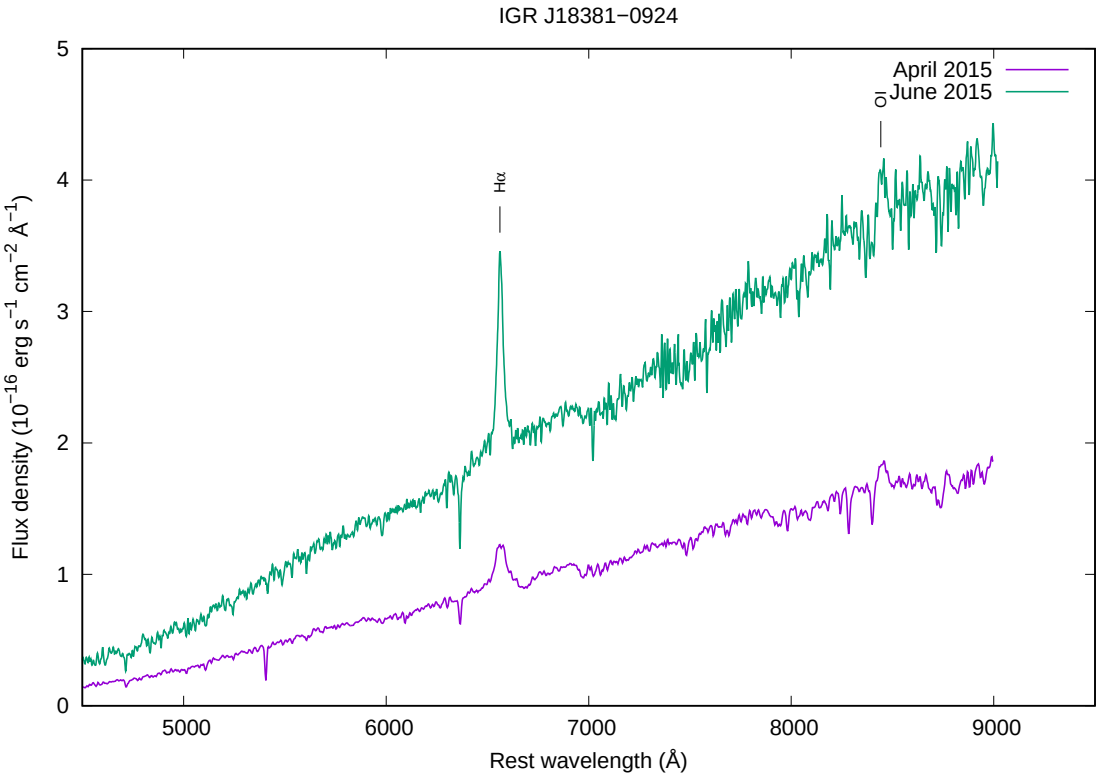

Figure 5. Rest-frame flux-calibrated FORS2 spectrum of IGR J18381−0924 observed in April 2015 (magenta) and June 2015 (green). All the detected emission lines are marked. The most prominent telluric absorption troughs were manually removed.

Table 3. Red-shifted optical emission lines in IGR J18381−0924 April and June 2015 FORS2 spectra.

		April 2015			June 2015		
Element	λ_c[a]	$\dot{W}$[b]	FWHM[c]	F_{line}[d]	$\dot{W}$	FWHM	F_{line}
Hα	6767	−26.4 ± 1.3	2614±224	2.41±0.13	−27.3 ± 0.6	1926 ± 102	4.87 ± 0.12
O I	8708	−4.8±1.2	1573±428	0.81±0.19	−4.8 ± 0.7	1571 ± 298	1.77 ± 0.25

[a]Measured wavelength in Å
[b]Equivalent widths in Å
[c]Full-width at half-maximum in km s^{-1}, quadratically corrected for instrumental broadening
[d]Intrinsic line flux in units of 10^{-15} erg cm^{-2} s^{-1}

that the value derived with *XMM-Newton* is lower than that obtained with *Chandra*, i.e. $(4 \pm 1) \times 10^{22}$ cm^{-2}, pointing towards variability. Correcting IGR J18381−0924 spectrum from this extinction, we measure an unabsorbed 1–10 keV flux of $(2.70 \pm 0.08) \times 10^{-12}$ erg cm^{-2} s^{-1}, whereas the absorbed 1–10 keV flux is $(2.30 \pm 0.06) \times 10^{-12}$ erg cm^{-2} s^{-1}.

Finally, we combined our PN and MOS data with the ISGRI one and fit the joint spectrum with the same model. The best fit is displayed in Figure 7 and the best-fit parameters are listed in the third column of Table 4. We obtain the very same results, proving that the *XMM-Newton* and *INTEGRAL* data are consistent. However, the ISGRI multiplicative constant compared to PN, $0.64^{+0.21}_{-0.19}$, is quite low, which likely stems fron the variability of the X-ray emission.

3.4 IGR J17164−3803

IGR J17164−3803 was detected by *INTEGRAL* with a 4.′2 positional accuracy (Krivonos et al. 2012) and we later observed it with ACIS on *Chandra*. We find six *Chandra* sources within the *INTEGRAL* error circle (see Table 5 in Tomsick et al. 2016b), five of them being very faint with 0.5–10 keV count rates between 1.0×10^{-3} and 2.4×10^{-3} count/s. Although we cannot rule out any of them as the actual soft X-ray counterpart to IGR J17164−3803, the latter would have to be either very hard, very absorbed, or variable to be that faint in the ACIS energy range (see Table 4 in Tomsick et al. 2016b). In contrast, the sixth source, which we consider as the most likely counterpart in the following, is brighter, with 5.7×10^{-3} count/s, and is also the second closest to the *INTEGRAL* position, with RA=17^h 16^m 26.97^s and DEC=−38° 00′ 07.8″ (Eq. J2000) for a 0.″73 uncertainty. We fit its 0.5–10 keV spectrum with anl absorbed power law, again for the Wilms et al. (2000) abundances and Verner et al. (1996) cross-sections, and we

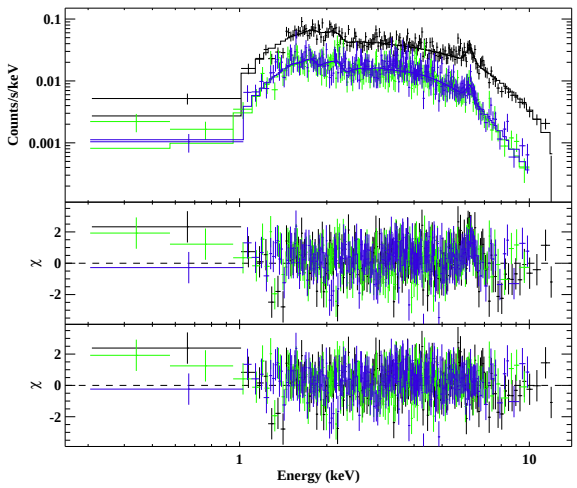

Figure 6. (Top) PN (black), MOS1 (green) and MOS2 (blue) *XMM-Newton* best-fit spectra of IGR J18381−0924. **(Middle)** Residuals for an absorbed power law, pointing towards the presence of an emission line between 6 and 7 keV. **(Bottom)** Residuals for an absorbed power law combined with a Gaussian centred around 6.24 keV.

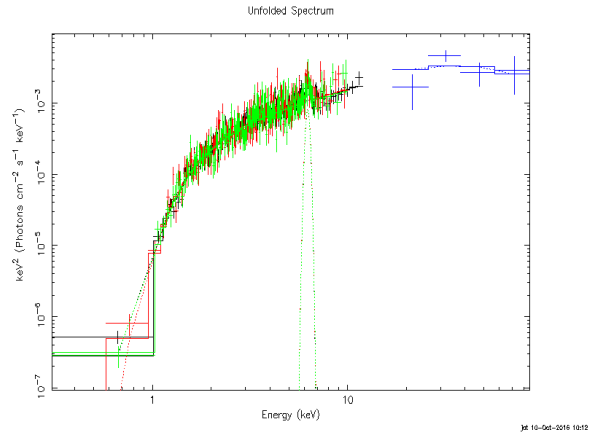

Figure 7. Best fit of the *XMM-Newton*/PN and *INTEGRAL*/ISGRI joint spectrum of IGR J18381−0924. The model used in a cutoff power law combined to a red-shifted iron line, both modified by photoelectric absorption.

derive $N_{\rm H} = 1.0^{+2.4}_{-1.0} \times 10^{22}$ cm^{-2} and $\Gamma = 1.0^{+1.3}_{-1.0}$, which points towards a relatively hard X-ray spectrum.

The accurate soft X-ray position allowed us to pinpoint its bright low energy counterpart, which we unambiguously associate with USNOB1.0 0519−0593639. The left panel of Figure 8 displays its FORS2 spectrum, which consists in a red continuum dominated by TiO molecular troughs as well as the Ca II triplet in absorption. Overall, it resembles that of an early M giant star, and a comparison with several observed templates provided by Le Borgne et al. (2003) shows that it is very likely an M2 III star with an approximate ISM extinction $A_{\rm V} \approx 4.6$ (Figure 8, right panel). We note that this value is roughly on par with the 3.5 to 5.5 estimate we find from DIB5779 equivalent width, the large range being due to the low resolution of our April spectrum. It also points towards USNOB1.0 0519−0593639 to be roughly located at 3 to 4 kpc.

Table 4. Best-fit parameters to the IGR J18381−0924 *XMM-Newton*/PN+MOS (left) as well as *XMM-Newton*/PN+MOS and *INTEGRAL*/ISGRI (right) spectra with CONSTANT×TBABS×(PEGPWRLW+ZGAUSS).

	$N_{\rm H}{}^a$	2.21 ± 0.16	2.22 ± 0.16
	Γ^b	1.19 ± 0.07	1.19 ± 0.07
	$E^c_{\rm iron}$	$6.24^{+0.05}_{-0.09}$	$6.24^{+0.05}_{-0.09}$
b	$\sigma^d_{\rm iron}$	$0.15^{+0.18}_{-0.07}$	$0.15^{+0.19}_{-0.07}$
	z^e	$0.026^{+0.016}_{-0.008}$	$0.026^{+0.016}_{-0.008}$
	$C^f_{\rm MOS1}$	1.00 ± 0.05	$1.00^{+0.04}_{-0.05}$
	$C^g_{\rm MOS2}$	0.96 ± 0.04	0.96 ± 0.04
	$C^h_{\rm ISGRI}$	–	$0.64^{+0.21}_{-0.19}$
c	F^i_{1-10}	2.3 ± 0.08	–
	$\chi^2_{\rm r}$ (d.o.f)	1.00 (582)	1.01 (584)

[a]Column density in units of 10^{22} cm^{-2}
[b]Power law photon index
[c]Iron line energy (keV)
[d]Iron line width (keV)
[e]Redshift
[f]MOS1 multiplicative constant
[g]MOS2 multiplicative constant
[h]ISGRI multiplicative constant
[i]1-10 keV absorbed flux in units of 10^{-12} erg cm^{-2} s^{-1}

4 DISCUSSION

We find that (1) IGR J18088−2741 optical spectrum is that of an optically thick accretion disc; (2) the same can be said for one of the two possible counterparts of IGR J19173+0747, the other one being an F3 V star; (3) IGR J18381−0924 is a variable extragalactic source with $z \approx 0.031$ red-shifted Hα and O I λ8446 emission lines; and (4) IGR J17164−3803 optical counterpart is an M2 III star.

Among the four sources, IGR J18088−2741 is that with the most unambiguous identification. Besides its optical spectrum, its other properties, i.e. an X-ray emission best-described by a hard cut-off power law, the presence of pulsations, as well as that of orbital modulations leave little doubts that the source is a magnetic CV, as already suggested in Tomsick et al. (2016b).

Likewise, the $z \approx 0.031$ red shift and hard *XMM-Newton* continuum suffering from a column density slightly in excess of the total Galactic extinction along its line-of-sight point towards IGR J18381−0924 being an obscured AGN. Based on the presence of broad Hα and O I λ8446 emission signatures, we tentatively classify the source as a type 1 galaxy in which we have a direct view of the broad emission line region (BELR). We note that O I is typical of a relatively dense region within the BELR with $n_{\rm h} \sim 10^{12}$ cm^{-3} in which Lyβ resonance fluorescence and collisional processes are important (see, e.g., Grandi 1980; Rodríguez-Ardila et al. 2002; Matsuoka et al. 2007). At this relatively low red shift, and taking into account the absence of a broad Hβ component, this would suggest a Seyfert 1.9 nature (Osterbrock 1981). It is however puzzling that no narrow forbidden emission lines are detected, as expected in Seyfert galaxies (see, e.g., Lee et al. 2013), but this may be due to the low X-ray luminosity of the source, i.e. 6.7×10^{42} erg s^{-1}, which we estimate from our X-ray fit between 1 and 10 keV. Moreover, the strong optical continuum variability, i.e. a factor 2 increase in 2 months, points towards the presence of an irradiated accretion disc,

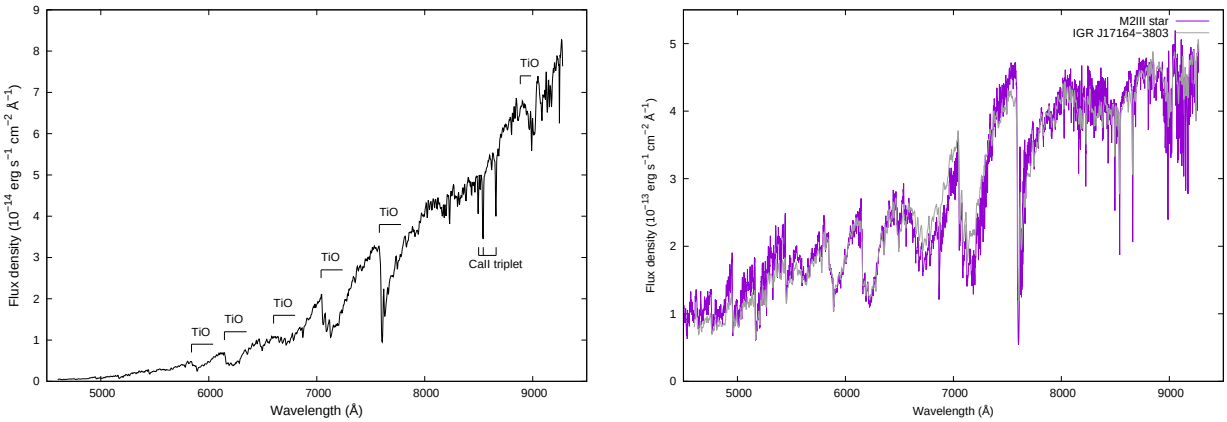

Figure 8. Left: flux-calibrated FORS2 spectrum of USNOB1.0 0519−0593639, the tentative optical counterpart to IGR J17164−3803. **Right:** Comparison of USNOB1.0 0519−0593639 FORS2 spectrum, corrected from an $A_V \approx 4.6$ ISM extinction, with that of a very weakly-extincted M2 giant star.

similarly to what is seen for NGC 5548 (see, e.g., McHardy et al. 2014).

Unlike the two previous sources, which have well-defined optical counterparts, IGR J19173+0747 *Swift* position is consistent with two objects. S1 exhibits the optical spectrum of an optically thick accretion disc with a flat Balmer decrement, which is usually found in CVs. The best-fit to the X-ray spectrum of the source, i.e. a hard cut-off power law, is also consistent with a CV and this is the reason why we favour S1 as the optical counterpart of IGR J19173+0747. We however cannot completely rule out S2, even if it is very difficult to see how an isolated F3 V star could be responsible for IGR J19173+0747 X-ray emission. Indeed, using the measurement given in Pavan et al. (2011) for the minimum 3 kpc distance derived in the present study, we find that the absorbed luminosity is about 6×10^{30} erg s^{-1}, which is 2 to 3 orders of magnitude larger than the X-ray luminosity expected from the coronal activity of such a star (see, e.g., Schmitt 1997), even without extinction correction. Alternatively, the star could be the companion of a compact object in a completely quiescent X-ray binary (XRB), which would reach such X-ray luminosity levels. For instance, the F6 IV/V star in GRO J1655-40 was shown to fully dominate the system in quiescence (Orosz & Bailyn 1997; Foellmi et al. 2006). Nonetheless, quiescent BH-XRBs are usually found to have a relatively soft power law-like X-ray spectrum with $\Gamma \approx 2$, without any cut-off, and quiescent NS-XRBs have an X-ray spectrum dominated by the NS surface. It would moreover be an extraordinary coincidence to find a CV and an XRB within less than 3″ from each other, perhaps located at the same distance. As such, we thus conclude that IGR J19173+0747 is very likely to be a CV, contradicting its previous classification as an HMXB.

The optical spectrum of the most likely soft X-ray counterpart to IGR J17164−3803 is fully consistent with an isolated M2 III star. We carefully searched for emission lines that could prove the presence of an accretion stream but could not find any. This however does not rule out the possibility that it is the companion of a compact object. Indeed, it is very unlikely that an isolated M star would be detected by *INTEGRAL*. This statement is strengthened when considering that the 0.5–10 keV flux we derive, 2.0×10^{-13} erg cm^{-2} s^{-1}, is equivalent to a luminosity of about 2.2×10^{32} erg s^{-1} for a minimum 3 kpc distance, respectively, a level which would be abnormally high for coronal emission from an isolated low mass star (see, e.g., Güdel & Nazé 2009). Likewise, the relatively hard power law best-fit to the *Chandra* spectrum is not consistent with the expected soft X-ray emission from an isolated early M giant (see, e.g., Rahoui et al. 2014; Fornasini et al. 2014). Instead, we rather believe that the most likely soft X-ray counterpart to IGR J17164−3803 is an X-ray faint symbiotic star, i.e. a white dwarf (WD) fed by the wind of its M2 III companion. The absence of shell-burning could lead to very weak optical emission lines undetectable through low-resolution spectroscopy, as recently proposed to explain the relatively bright hard X-ray emission of an M giant star thought to be isolated, SU Lyncis (Mukai et al. 2016). The authors argue that a potentially large population of such systems could be present in the Galaxy, leading to an underestimation of the known symbiotic stars. Although we stress that we may have picked the wrong soft X-ray counterpart, we believe that IGR J17164−3803 is a new member of this family.

5 CONCLUSION

We have reported on FORS2 spectroscopy of the optical counterparts of four IGR sources, the X-ray properties of which were consistent with what we expect from the elusive HMXBs that host BHs instead of NSs. We show that none of them is an actual HMXB, as IGR J18088−2741 and IGR J19173+0747 are magnetic CVs, IGR J18381−0924 is a faint Seyfert 1.9 galaxy, and IGR J17164−3803 is, perhaps, a faint symbiotic star. On the one hand, our results illustrate the efficiency of ever-deeper X-ray surveys with soft and hard X-ray facilities such as *Chandra* and *INTEGRAL* in unveiling new populations of X-ray emitters with relatively hard X-ray spectra, in particular faint magnetic CVs and wind-accreting symbiotic stars. On a longer term, this will likely help us refine what we know about these sources and, perhaps, challenge current accepted schemes. However, our study also points towards the difficulty of identifying HMXBs , in particular SGXBs, and highlights the limitations of the accepted selection criteria of HMXB candidates – a Galactic plane location, a hard X-ray spectrum, and a variable X-ray emission – which must be revisited. It is thus likely that many hard X-ray sources thought to be HMXB candidates based on these criteria have another nature. If true, this should be taken into account in HMXBs and BH-BH population synthesis models. Likewise, the detection of new BH-HMXBs probably requires very sensitive hard X-ray instruments, as we expect them to be very weak accretors (see, e.g., Zhang et al. 2004;

Casares et al. 2014; Munar-Adrover et al. 2014). This is the reason why we favour the use of an hard X-ray observatory such as the *Nuclear Spectroscopic Telescope Array* (*NuSTAR*, Harrison et al. 2013), combined with state-of-the-art infrared spectroscopic facilities, to determine whether or not a significant population of BH-HMXBs exists in our Galaxy.

ACKNOWLEDGEMENTS

We thank the referee for his/her comments and time committed to the correction of this work. FR thanks the ESO staff who performed the service observations. JAT acknowledges partial support from NASA under *XMM-Newton* Guest Observer grant NNX15AW09G. RK acknowledges support from Russian Science Foundation through grant 14-22-00271. This research has made use of data obtained from the High Energy Astrophysics Science Archive Research Center (HEASARC), provided by NASA's Goddard Space Flight Center. This research has made use of NASA's Astrophysics Data System, of the SIMBAD, and VizieR databases operated at CDS, Strasbourg, France.

REFERENCES

Abbott B. P., et al., 2016, Physical Review Letters, 116, 061102
Appenzeller I., et al., 1998, The Messenger, 94, 1
Belczynski K., Ziolkowski J., 2009, ApJ, 707, 870
Bird A. J., et al., 2016, ApJS, 223, 15
Bodaghee A., Rahoui F., Tomsick J. A., Rodriguez J., 2012, ApJ, 751, 113
Burrows D. N., et al., 2005, Space Sci. Rev., 120, 165
Casares J., Negueruela I., Ribó M., Ribas I., Paredes J. M., Herrero A., Simón-Díaz S., 2014, Nature, 505, 378
Chaty S., Rahoui F., 2012, ApJ, 751, 150
Chaty S., Rahoui F., Foellmi C., Tomsick J. A., Rodriguez J., Walter R., 2008, A&A, 484, 783
Coleiro A., Chaty S., Zurita Heras J. A., Rahoui F., Tomsick J. A., 2013, A&A, 560, A108
Fitzpatrick E. L., 1999, PASP, 111, 63
Foellmi C., Depagne E., Dall T. H., Mirabel I. F., 2006, A&A, 457, 249
Fornasini F. M., et al., 2014, ApJ, 796, 105
Freudling W., Romaniello M., Bramich D. M., Ballester P., Forchi V., García-Dabló C. E., Moehler S., Neeser M. J., 2013, A&A, 559, A96
Gehrels N., et al., 2004, ApJ, 611, 1005
Grandi S. A., 1980, ApJ, 238, 10
Green G. M., et al., 2015, ApJ, 810, 25
Güdel M., Nazé Y., 2009, A&A~Rev., 17, 309
Güver T., Özel F., 2009, MNRAS, 400, 2050
Harrison F. A., et al., 2013, ApJ, 770, 103
Jansen F., et al., 2001, A&A, 365, L1
Jenniskens P., Desert F.-X., 1994, A&AS, 106, 39
Krivonos R., Tsygankov S., Lutovinov A., Revnivtsev M., Churazov E., Sunyaev R., 2012, A&A, 545, A27
Le Borgne J.-F., et al., 2003, A&A, 402, 433
Lee J. C., et al., 2013, MNRAS, 430, 2650
Lucas P. W., et al., 2008, MNRAS, 391, 136
Marshall D. J., Robin A. C., Reylé C., Schultheis M., Picaud S., 2006, A&A, 453, 635
Masetti N., et al., 2012, A&A, 538, A123
Matsuoka Y., Oyabu S., Tsuzuki Y., Kawara K., 2007, ApJ, 663, 781
McHardy I. M., et al., 2014, MNRAS, 444, 1469
Minniti D., et al., 2010, NewA, 15, 433
Mukai K., et al., 2016, MNRAS, 461, L1
Munar-Adrover P., Paredes J. M., Ribó M., Iwasawa K., Zabalza V., Casares J., 2014, ApJL, 786, L11
Negueruela I., Smith D. M., Reig P., Chaty S., Torrejón J. M., 2006, in Wilson A., ed., ESA Special Publication Vol. 604, The X-ray Universe 2005. pp 165–170
Orosz J. A., Bailyn C. D., 1997, ApJ, 477, 876
Osterbrock D. E., 1981, ApJ, 249, 462
Pavan L., Bozzo E., Ferrigno C., Ricci C., Manousakis A., Walter R., Stella L., 2011, A&A, 526, A122
Rahoui F., Chaty S., 2008, A&A, 492, 163
Rahoui F., Chaty S., Lagage P.-O., Pantin E., 2008, A&A, 484, 801
Rahoui F., Tomsick J. A., Fornasini F. M., Bodaghee A., Bauer F. E., 2014, A&A, 568, A54
Rodríguez-Ardila A., Viegas S. M., Pastoriza M. G., Prato L., Donzelli C. J., 2002, ApJ, 572, 94
Schmitt J. H. M. M., 1997, A&A, 318, 215
Soszyński I., et al., 2011, Acta Astron., 61, 1
Strüder L., et al., 2001, A&A, 365, L18
Tomsick J. A., Chaty S., Rodriguez J., Walter R., Kaaret P., 2008, ApJ, 685, 1143
Tomsick J. A., Bodaghee A., Chaty S., Rodriguez J., Rahoui F., Halpern J., Kalemci E., Özbey Arabaci M., 2012, ApJ, 754, 145
Tomsick J. A., Rahoui F., Krivonos R., Clavel M., Strader J., Chomiuk L., 2016a, MNRAS, 460, 513
Tomsick J. A., Krivonos R., Wang Q., Bodaghee A., Chaty S., Rahoui F., Rodriguez J., Fornasini F. M., 2016b, ApJ, 816, 38
Turner M. J. L., et al., 2001, A&A, 365, L27
Ubertini P., et al., 2003, A&A, 411, L131
Verner D. A., Ferland G. J., Korista K. T., Yakovlev D. G., 1996, ApJ, 465, 487
Weisskopf M. C., Brinkman B., Canizares C., Garmire G., Murray S., Van Speybroeck L. P., 2002, PASP, 114, 1
Williams R. E., 1980, ApJ, 235, 939
Wilms J., Allen A., McCray R., 2000, ApJ, 542, 914
Winkler C., et al., 2003, A&A, 411, L1
Zhang F., Li X.-D., Wang Z.-R., 2004, ApJ, 603, 663

This paper has been typeset from a TEX/LATEX file prepared by the author.